

Experimental and Numerical Analysis of Vertical Axis Wind Turbine

Dr. Prashant W. Deshmukh¹, Mr. Shrikant D. Hade², Mr. Hrushikesh M. Hiwase³

¹College of Engineering Pune, Pune-05,
Shivajinagar, Pune, Maharashtra 411005,
pwdeshmukh25@gmail.com

²Pune Institute of Computer Technology, Pune-43
Near Trimurti Chowk, Dhankawadi, Pune,
sdhade@pict.edu

³Pune Institute of Computer Technology, Pune-43
Near Trimurti Chowk, Dhankawadi, Pune,
hmhiwase@pict.edu

Abstract: The Vertical Axis Wind Turbine (VAWT) is an effective energy harnessing device in comparison with Horizontal Axis Wind Turbines (HAWT). The focus of the present study is to obtain a rotor blade shape that gives a high power at minimum wind velocity, minimum starting torque, and minimum cut-in wind speed. Simulation of the model uses the different wind speeds to determine the performance of the wind turbine. A 1200 mm high and 1000 mm swing diameter turbine includes eight blades. An experimental study is carried out for two different blade shapes viz. U-shaped blade and the Fan type blade. Experimental results are presented for different airflow velocities in terms of Revolutions per minute (RPM) of the rotor, the force exerted, and torque required to attain a specific rotor speed. The experimental results reveal that the fan-type blade gives better performance than U type blade. Power characteristics are also studied for the Fan type blade rotor. The numerical study confirms the experimental results for fan type blade rotor. FAN type blades are analyzed for the different bend angles from 130° to 140°.

Keywords: VAWT, fan type blade, bend angle, U shape blade.

(Article history: Received: 17th April 2021 and accepted 13th June 2021)

INTRODUCTION

Wind energy the fastest-growing alternative energy source in the world, it offers many advantages. A wind turbine or wind generator is a rotating machine that converts the kinetic energy of wind into mechanical energy which can further be converted to generate electricity. Wind energy is a clean and inexhaustible fuel source, fueled by the wind, which in turn is fueled by the sun. Wind energy does not pollute the atmosphere like conventional power plants which rely on fossil fuels like coal or gas. If we harness wind energy which is a clean source of energy, it will reduce our dependency on fossil fuels to decrease CO₂ emission into the atmosphere.

Horizontal axis wind turbine (HWAT) is the most common type of wind turbine that is used nowadays. The geometry (shape and size) i.e. a profile of the blade is the most important factor which determines the amount of energy extracted from the wind. Generally,

wind turbines are classified into two types based on the axis in which the turbine axis rotates. Turbines that rotate around a horizontal axis are referred to as horizontal axis wind turbines (“HAWT”). They are the most common type of wind turbine in use today and are typically seen in open spaces along highways. Turbines that rotate around a vertical axis are referred to as vertical axis wind turbines (“VAWT”) and are less frequently used because they are less efficient.

Vertical axis wind turbines (VAWT’s) is having a main rotor shaft and blades arranged vertically. Some of the advantages of this system are that the turbine is not required to be pointed into the wind to be effective; they work with wind from any direction. This proves to be much advantageous in locations where wind direction is highly variable. VAWT are installed on the ground or rooftop of a building; they can also be mounted at top of tall towers with all the gear (winding coil gearbox and generator) at ground level. This can provide the advantage of easy accessibility to mechanical

components for installation and maintenance. Also, VAWT designs do not require a yaw mechanism or extra motors to turn into the wind.

Carrigan et al (1) did optimization of aerofoil cross-section by using a completely automated process. He used DE algorithm which was subjected to TIP Speed Ratio, design constraints of blade profile, and Solidity. This optimization process resulted in an optimized cross-section of the blade for two test cases, which was resulted in designs with higher efficiency. Abdulkadir Ali et al (2) studied VAWT for partially cowled configuration with two blade sets made from steel and cardboard. This analysis shows that for partially cowled configuration of cardboard made turbine rotational motion is high. It also shows that lighter turbines give good performance. W. T. Chang et al (3) used VAWT integrated Omni-Directional Guide Vane (ODGV) which improved the self-starting of VAWT. At the condition of free-running rotor speed was increased by 182% & power output was 3.48 times higher at the maximum torque compared to normal VAWT.

S. Mc Tavish et al (4) used RANS CFD simulation to assess the performance of novel VAWT. He conducted a steady & rotating validation study for Savonius rotor using experimental data. This study resulted in comparable amount of static torque is produced by Aeolun Harvester to the existing savonius rotor. Huimin Wang et al (5) studied a 2D model of VAWT at different velocities of wind. This resulted in, increasing the wind velocity variation in turbines total torque coefficients tends to smooth. Parvez et. al. (6) analyzed the performance of the airfoil NACA 4518; he presented flow structure for the complex unsteady analysis of VAWT. The performance parameter which is the coefficient of lift is presented for different angle of attacks. The coefficient of lift is the most important result for the simulation. The airfoil was subjected to a variable angle of attack both in a positive and negative direction. Sukantaroy et al (7) did 2D unsteady simulation to study the effect of overlap ratios on static torque of a drag-based VAWT. In this study realizable K-turbulence model proved to be superior out of various K-turbulence tested models. H. Beri et al (8) studied the NACA 0018 profile of the blade. This

I. EXPERIMENTAL SETUP AND METHODOLOGIES

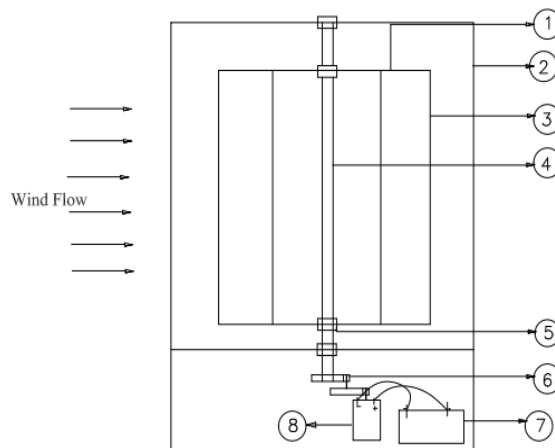
The block diagram of the experimental test apparatus is shown in Fig. 1, consists of a metal frame, rotor plate,

resulted in, for lower tip speed ratios turbine generates negative torque with DMST simulation & the turbine generated positive torque for lower Tip Speed Ratios with CFD simulation. J. T. Hansen et al (9) conducted a numerical study of VAWT. In this study, he concluded that mesh size domain cell density, number of iterations per time step, and azimuth increment have the biggest impacts on results. S. B. Qamar et al (10) investigated cambered blades for VAWT using CFD. He concluded that AWT with cambered blades gives a better performance coefficient, this arrangement is also found effective at low wind speeds. D. W. Wekesa et al (11) studied two VAWT configurations H-type & Savonius type to compare its aerodynamics performance. This resulted in drag-based Savonius rotors has low aerodynamic efficiency than lift-based Darrius VAWT rotors. For small-scale VAWT rotors, a nonuniform turbulent flow improves its self-starting capacity. M. S. Siddiqui et al (12) investigated rooftop VAWT with respect to ground clearance this resulted in more ground clearance yielded in maximum efficiency. J. U. Parakkal et al (13) used H-rotor for analysis of VAWT. He has used Joukowski airfoil. Assessment of result was based on lift coefficient, torque, and power coefficient using CFD. The use of Joukowski airfoil resulted in improvement of torque which adversely affected the self-starting behavior of VAWT. M. K. Rathore et al (14) proposed the use of wind energy produced from vehicle movement on the highway, he used waste material i.e. plastic drum to design VAWT which resembles like Savonius type VAWT. T. M. Premkumar et al (15) carried out performance test of helical Savonius type VAWT with and without endplates. He observed that performance of helical Savonius type VAWT having endplate was better than without endplate.

The objective of the present work is to design a compact VAWT for the generation of maximum electricity with minimum input wind velocity. The work also extended for investigation of its performance at different wind speeds, different rotor blade shapes viz. U-shape blade and Fan type profile, different blade bend angle.

rotor shaft, bearings, rotor blades, gears, 12V DC alternator, and 12V battery. The metal frame is fabricated with the help of a mild steel angle plate 1800 mm high and 1400 mm length structure. The rotor shaft

is connected to the frame with the help of bearings; it is the main shaft around which the blades rotate. To provide support to the blade's circular plates (rotor plate) are used at the top and bottom of the rotor; it is made of mild steel with 1000 mm diameter. Space between the rotor plates encompasses the wind turbine blades. The capacity of the turbine to give more rotations depends upon the weight of the turbine, which is related to the weight of the blade for this reason aluminum is selected for the fabrication of the blades as it is very light in weight. The height and width of the blade are taken as 1200 mm and 1000 mm, respectively. To obtain the high range of rotations and to transmit the rotations of the rotor shaft to the alternator shaft gears are used. A gear with 60 teeth is mounted on the rotor shaft it is connected to a gear with 12 teeth on the same shaft gear with 60 teeth is mounted which is then coupled with the gear mounted on the rotor shaft which has 12 teeth. A 12V DC alternator is used to convert mechanical energy to electrical energy; it can sustain the 1500 RPM and can generate a current up to 14A and voltage up to 14V. Positive and negative terminals of the alternator are attached to the respective terminals of the battery. This assembly of the rotor is then tested on 30 feet high rooftop of a building. The instantaneous wind velocity is measured by a calibrated anemometer, and average wind velocity is considered for the experimental calculations. The revolutions of the rotor are measured with the help of calibrated tachometer. A multimeter is used for the measurement of current and the voltage through the alternator.



1 – Rotor Plate, 2 – Metal Frame, 3 – Turbine Blade, 4 – Rotor Shaft, 5 – Bearings, 6 – Gear, 7 – Battery, 8 – Alternator

Fig. 1: Block diagram of the experimental setup



Fig.2: Fan type turbine mounted over the set-up

TABLE 1: SPECIFICATIONS OF BLADE

Description	Dimensions
Height of the blade (H)	1200 mm
Width of the blade for Fan type rotor (W)	330 mm
Circumference of the blade (U shaped blade)	330 mm

Thickness of the blade (t)	2 mm
Diameter of a rotor (D)	1000 mm
Bend angle of blades for Fan type rotor	135 ⁰
Projected Area (a)	3.168 m ²
Swept area ($A=D \times H$)	1.2 m ²

TABLE 2: MATERIAL USED FOR PARTS OF TURBINE

Part Name	Material
Metal Frame	Mild Steel (MS) Angle Plate
Blades	Aluminum Sheet
Shaft	Mild Steel (MS)
Rotor	Mild Steel (MS)

The test section is first tested for the free rotations of the rotor, and certain required adjustments are done to ensure no play between the rotor plate and the main rotor shaft. The startup wind turbine speed is a minimum wind speed required to overcome the frictional force & inertia of the system, and to bring the rotor to a state of free rotation. Therefore, the experimental setup initially tested for the wind velocity at which it gives first rotation. The next step was to measure the rotations of the rotor shaft at varying wind velocities. Further, wind velocity and corresponding rotor rotations are measured at which the alternator generates the current.



Fig. 3: Electrical set-up to convert mechanical power to electrical power.

Figure 3 shows the experimental setup of the wind turbine. The full-scale turbine is tested for wind speeds

up to 4.5 m/s. Initially, the wind speed at which the turbine started rotating was recorded. During the test, it was observed that after the turbine starts rotating, it would continue to rotate even at lower wind velocity than at which it began to rotate initially.

The experimental study is carried out for a wind turbine with two different blade profiles i.e. ‘U’, and Fan shape with different bend angles. These two blade profiles are analyzed for their capacity of revolutions per minute, torque, and electrical power generation with available input wind speed. The fan rotor profile was experimentally tested and analyzed in commercial CFD software for confirmation of experimental results. Additionally, this blade profile with three different blade bend angles was studied numerically for three bend angles.

The terminology used for wind turbine:

The swept area of rotor:

$$\text{The swept area of the rotor} - A = D \times H$$

Wind power:

The power available in a free-flowing wind stream of cross-sectional area, A is

$$P_{wind} = (\text{Volume flow rate}) \times (\text{Kinetic energy per unit volume})$$

$$P_{wind} = (A \times V) \times (0.5 \times \rho \times V^2)$$

$$P_{wind} = (0.5 \times m \times V^2) \tag{2}$$

Assuming air to be a stable mixture of perfect gases, the air density, ρ can be derived from the Perfect gas equation as:

$$\rho = P/R.T \tag{3}$$

Coefficient of performance (C_p):

The coefficient of performance is defined as the ratio of power extracted by a wind turbine to the total power available in the cross-sectional area of the wind stream subtended by the wind turbine.

$$C_p = P_{Turbine} / P_{wind} \tag{4}$$

The power extracted by a wind turbine:

$$P_{Turbine} = C_p \cdot (0.5 \times \dot{m} \times V^2) \tag{5}$$

The parameter CP fundamentally represents mechanical efficiency which accounts for the performance of different mechanical parts of the system, and its maximum value of 0.593 is proved using the Betz’ law.

II. RESULT AND DISCUSSIONS

The experimental assessment is made for the evaluation of wind turbine for different wind speeds. The blade profile improves the performance of a wind turbine at the optimum speed for maximum efficiency. Table 3 shows the performance characteristics of the VAWT. However, the performance results are only of the turbine rotor and do not include the performance of the

coupled alternator. Further, since the power extracted by the rotor from the wind varies with air density, the power output of the wind rotor is obtained at different air velocities.

During the testing of the novel VAWT, the wind anemometer recorded a maximum wind speed of 5 m/s. However, there are very few samples of wind speed. above 4.5 m/s. Hence it was not considered statistically appropriate to include the data for wind speeds above 4.5 m/s for evaluating the power performance.

The field tests were carried out on the VAWT prototype with two different blade shapes. The data obtained from these test results were compiled and analyzed by using various tools as described in the previous chapter. This chapter presents the field test results in tabular as well as graphical form and includes a detailed analysis of the test results to reason out the trends obtained.

TABLE 3: EXPERIMENTAL RESULTS FOR FAN TYPE BLADE WITH BEND ANGLE 135° AND U-SHAPED BLADE

Wind Velocity, V (m/sec)	Rotor speed, N (rpm)	Rotor speed, N (rpm)	Angular velocity, ω (rad/sec)		Torque, T (N-m)		Force, F (N)	
	<i>U-Shaped Blade</i>	<i>Fan Type Blade</i>	<i>U-Shaped Blade</i>	<i>Fan Type Blade</i>	<i>U-Shaped Blade</i>	<i>Fan Type Blade</i>	<i>U-Shaped Blade</i>	<i>Fan Type Blade</i>
1	2	5	0.209	0.523	2.091	0.836	4.181	1.672
1.5	5	8	0.523	0.837	2.822	1.764	5.645	3.528
2	11	14	1.151	1.465	3.041	2.389	6.082	4.779
2.5	18	21	1.884	2.198	3.630	3.111	7.259	6.222
3	22	24	2.303	2.512	5.131	4.704	10.263	9.408
3.5	26	30	2.721	3.140	6.895	5.976	13.790	11.951
4	32	35	3.349	3.663	8.362	7.646	16.725	15.291
4.5	41	46	4.291	4.815	9.293	8.283	18.586	16.566

Table 4: Experimental results of fan type blade rotor of bend angle 135°

Wind Velocity, V (m/s)	Rotor speed, N (RPM)	ω/p rpm	Current, I (A)	Voltage, V (Volts)	Power _{el} (Watts)	p_{wind} (Watts)	P_{tur} (Watts)	angvel (rad/sec)	Torque (Nm)	Force (N)
1	5	125	0.988	12.41	12.261	0.73	0.437	0.523	0.836	1.67
1.5	8	200	2.3	12.41	28.543	2.49	1.477	0.837	1.763	3.52
2	14	350	3	12.41	37.23	5.90	3.501	1.465	2.389	4.77
2.5	21	525	4.4	12.41	54.604	11.53	6.838	2.198	3.111	6.22
3	24	600	8.2	12.41	101.762	19.92	11.816	2.512	4.703	9.40
3.5	30	750	12	12.41	148.92	31.64	18.763	3.14	5.975	11.95
4	35	875	13	13.32	173.16	47.23	28.008	3.663	7.645	15.29
4.5	46	1150	14.65	13.88	203.342	67.25	39.879	4.814	8.282	16.56

Figures 4 through 7 show the graphical representation of the novel VAWT. The various characteristic curves are as follows:

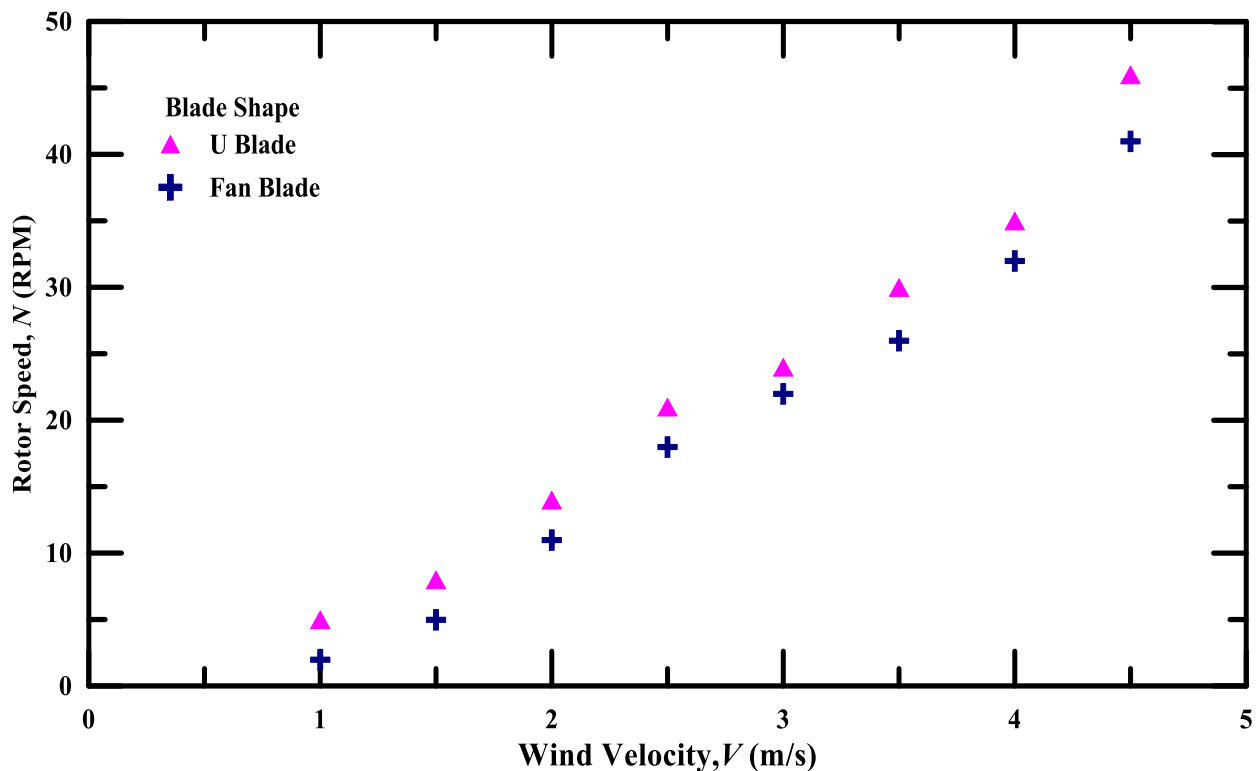


Fig.4: Variation of rotor speed, N with wind velocity, V

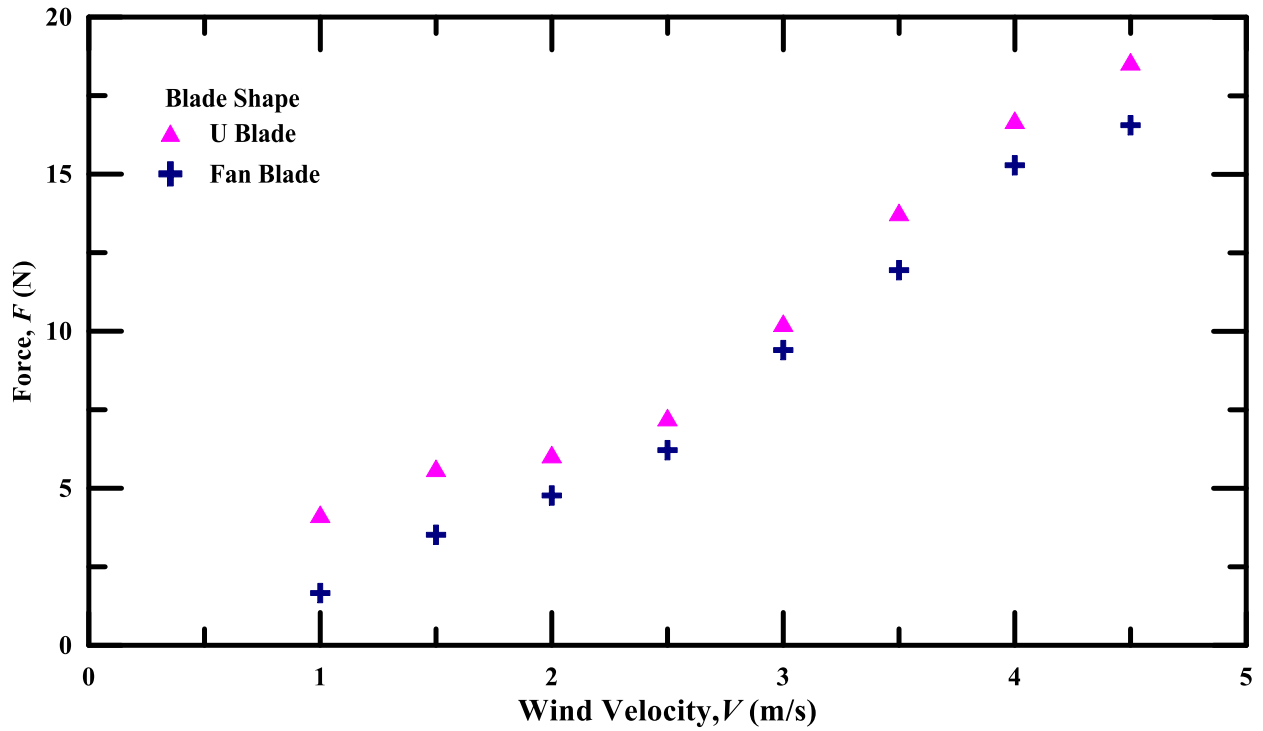


Fig. 5: Variation of force, F with wind velocity, V

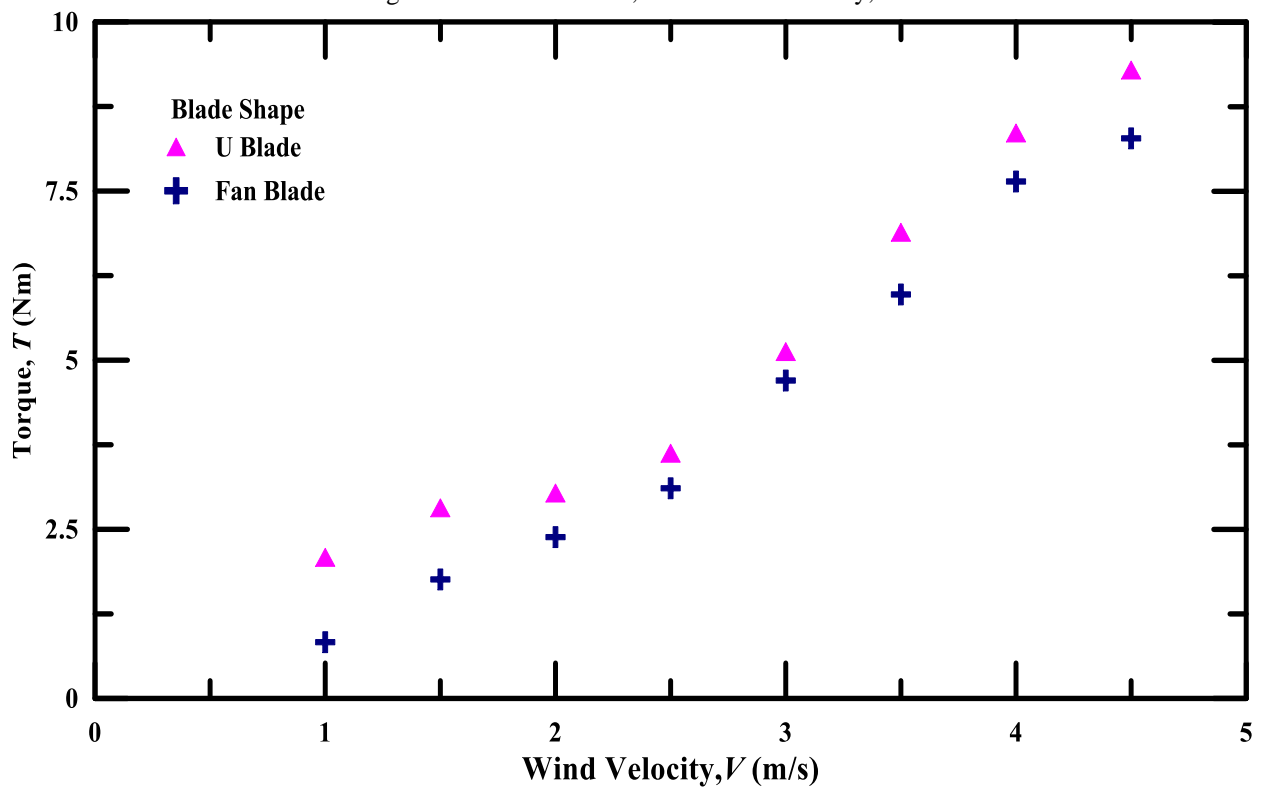


Fig. 6: Variation of shaft torque with wind velocity

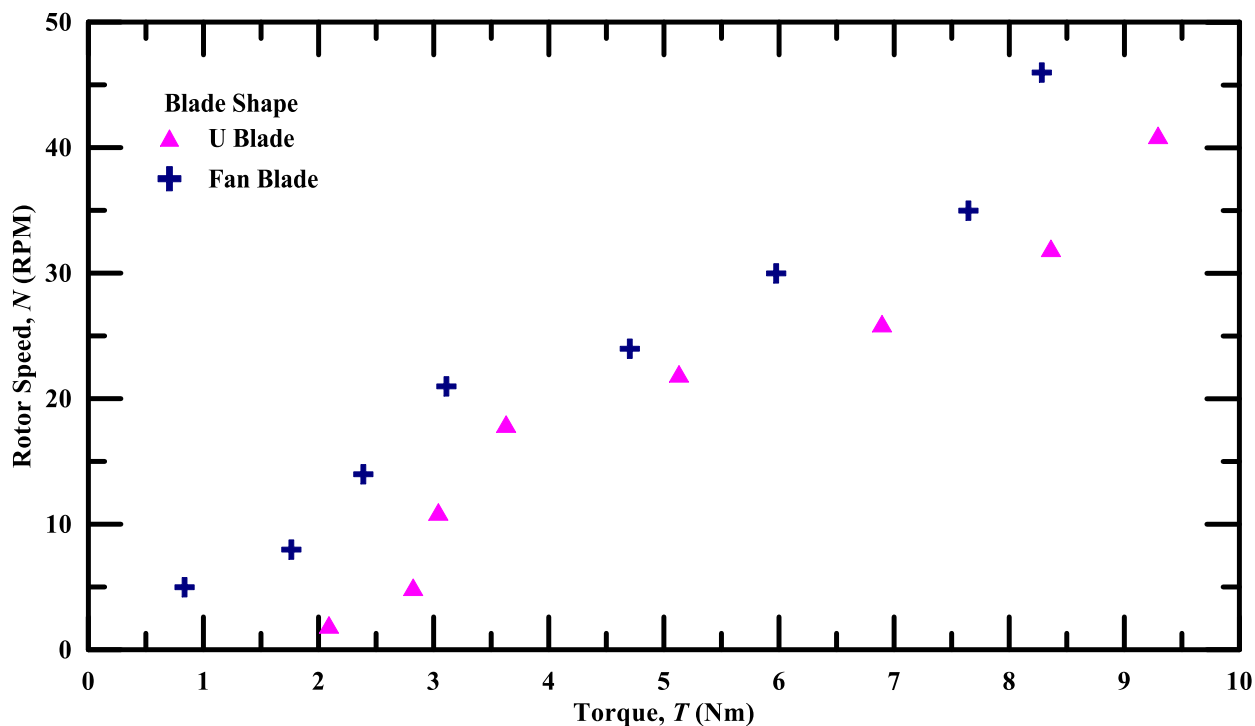


Fig.7: Variation of rotor speed with torque

Figure 4 to 7 shows the variation of the shaft torque, force, and rpm with respect to wind velocity for two blade configurations that is U-Shaped blade rotor and Fan type blade rotor. Both configurations are tested for a wide range of wind velocities varying from 0 m/s to 4.5 m/s.

From the above figure, it can be observed that U-shaped blade rotor highest recorded rotation is 41 rpm is whereas for the fan type blade it is 46 rpm, graphs also indicate that the former requires high torque to start its first rotation than the later this indicates that U-shaped blade rotor requires a comparatively high wind speed than Fan type rotor.

From graphs, it can also be observed that Fan type blade rotor starts its rotations at around 1.5 m/s wind velocity which is a cut in wind speed for the U- shaped blade rotor. Fan type blade rotor gives a reasonable rotation at around 3 m/s wind speed which is cut in wind speed for the many existing wind turbines.

Fig.8 shows the power curve for the Fan type turbine blade rotor, as can be seen from the fig the power extracted by the wind turbine varies depending upon the wind velocity and the RPM of a rotor. From the data, it can be observed that the RPM of the rotor is very less i.e. maximum of 46 rpm is recorded at the 4.5 m/s wind velocity which can be converted by using the high gear ratio.

During the test, it was observed that the 12V DC generator started generating the power at a wind velocity of 3.5 m/s at which rotor speed was recorded as 30 rpm and output rpm that is at the alternator was around 750. At this value, there occurs a cut-off and current flow from the alternator to the battery. The power curves for the Fan type blade VAWT as shown in the figure indicate that the power output of the turbine varied between 0 and 203.342 watts for wind speed ranging from 0 to 4.5 m/s. However, the turbine started generating power (rotations) at an average wind speed of 1.5 m/s, which is lower than the cut-in speeds

of most of the wind turbines currently available in the market. The cut-in wind speed usually ranges from 3 to 4 m/s. Further, the power output of the turbine steadily increased with wind speed, which is a usual trend.

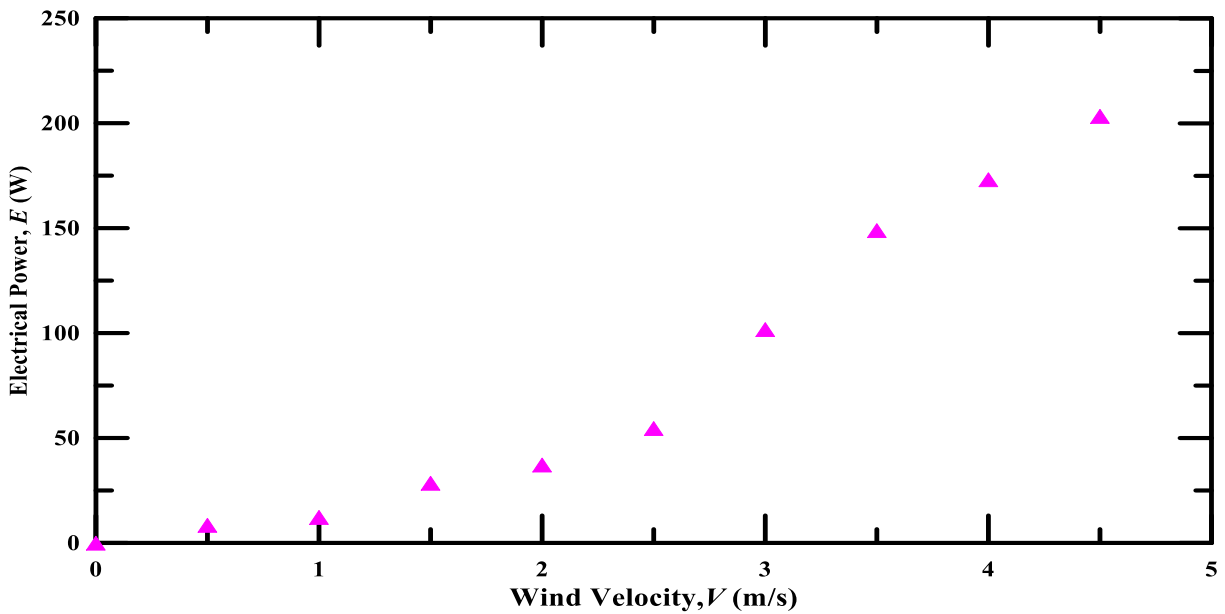


Fig. 8: Variation of electrical power, E with wind velocity, V

III. NUMERICAL STUDY

A CFD analysis of a fan-type bade rotor is carried out and is compared with the experimental values. For CFD analysis fluent gives the value of force in three directions viz. X, Y, Z the force acting on the rotor blade in the Z direction is almost equal to zero, this is

because the rotor is directed in a Z direction. Based on the value of force in the X and Y direction, the resultant force acting on the blades is calculated and is compared with the experimental value.

Table 5: Validation of experimental result with CFD result

Experimental values				CFD values			Error (%)
Velocity (m/s)	Rotor speed RPM	Torque (N-m)	Force (N)	F_x (N)	F_y (N)	Resultant force (N)	
1	5	0.836243	1.672487	1.38	1.19	1.822223916	8.27
1.5	8	1.763951	3.527901	1.74	3.48	3.890758281	9.32
2	14	2.389267	4.778533	4.12	3.33	5.27867	9.47
2.5	21	3.111024	6.222048	4.57	4.709	6.56197996	5.18
3	24	4.703869	9.407737	7.8	7.2	10.61508361	11.37
3.5	30	5.975655	11.95131	8.972	7.0723	11.42428165	4.40
4	35	7.645653	15.29131	12.41	6.34	13.93569876	8.86
4.5	46	8.282899	16.5658	16.07	8.1	17.99596899	7.94

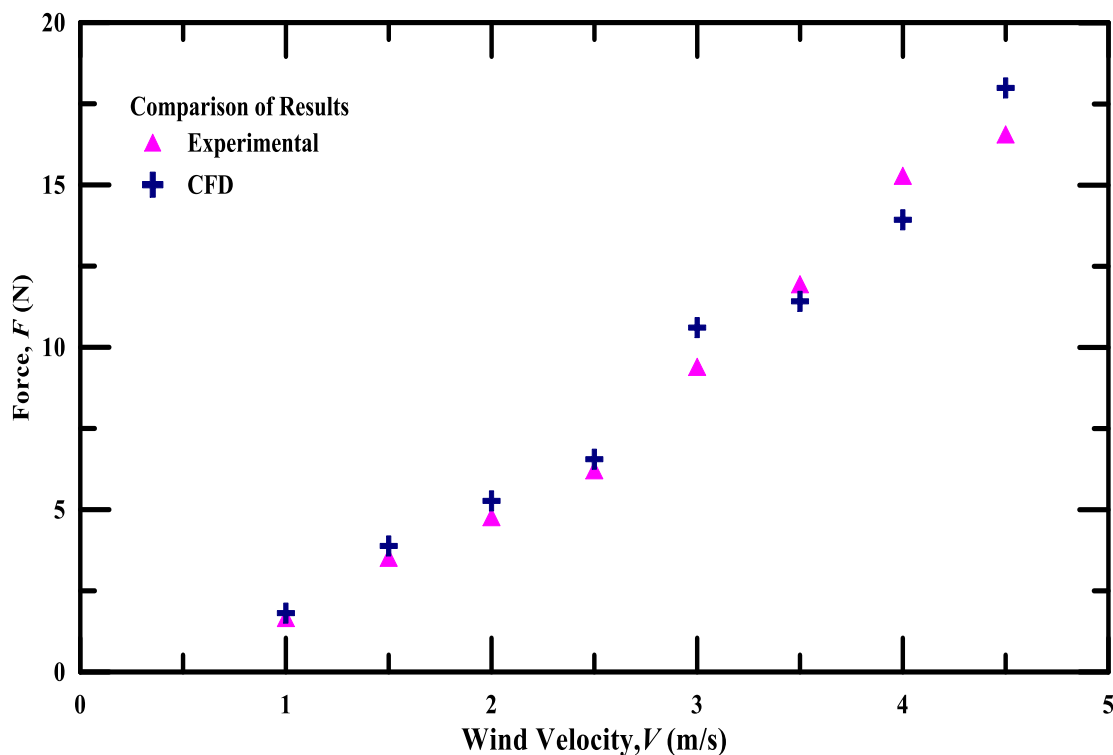


Fig. 9: Comparison of CFD and experimental values for rotor with 135° blade bend angle

After the validation of the experimental readings with the CFD for Fan type blade with bend angle 135°, two more cases are studied with bend angles 130° and 140°, and the effect of air velocity is analyzed by maintaining all the boundary conditions and the mesh size that are

used for the 135° bend angle blade. As discussed earlier that the blade which requires less force to generate the rpm at a given wind velocity therefore the two are analyzed to calculate the force acting on the blade for the given wind velocity.

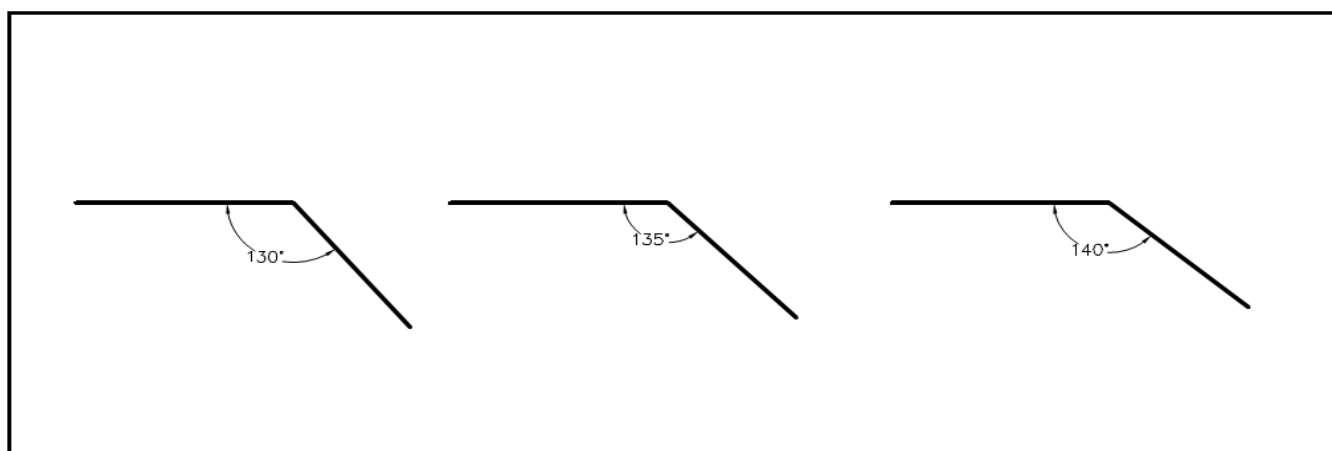


Fig. 10: Fan type blade with different bend angles

Table 6: CFD results for fan type blade with different bend angles

Wind Speed, (m/s)	Force (N)								
	Bend angle130°			Bend angle 135°			Bend angle140°		
	F _x	F _y	Resultant Force	F _x	F _y	Resultant Force	F _x	F _y	Resultant Force
3	7.24	13.63	15.43	7.8	7.2	10.61	9.48	9.63	13.51
3.5	10.36	13.15	16.74	8.972	7.0723	11.42	10.21	9.84	14.17
4	12.09	13.75	18.30	12.41	6.34	13.93	12.29	12.29	17.38
4.5	16.17	16.11	22.82	16.07	8.1	17.99	14.81	14.51	20.73

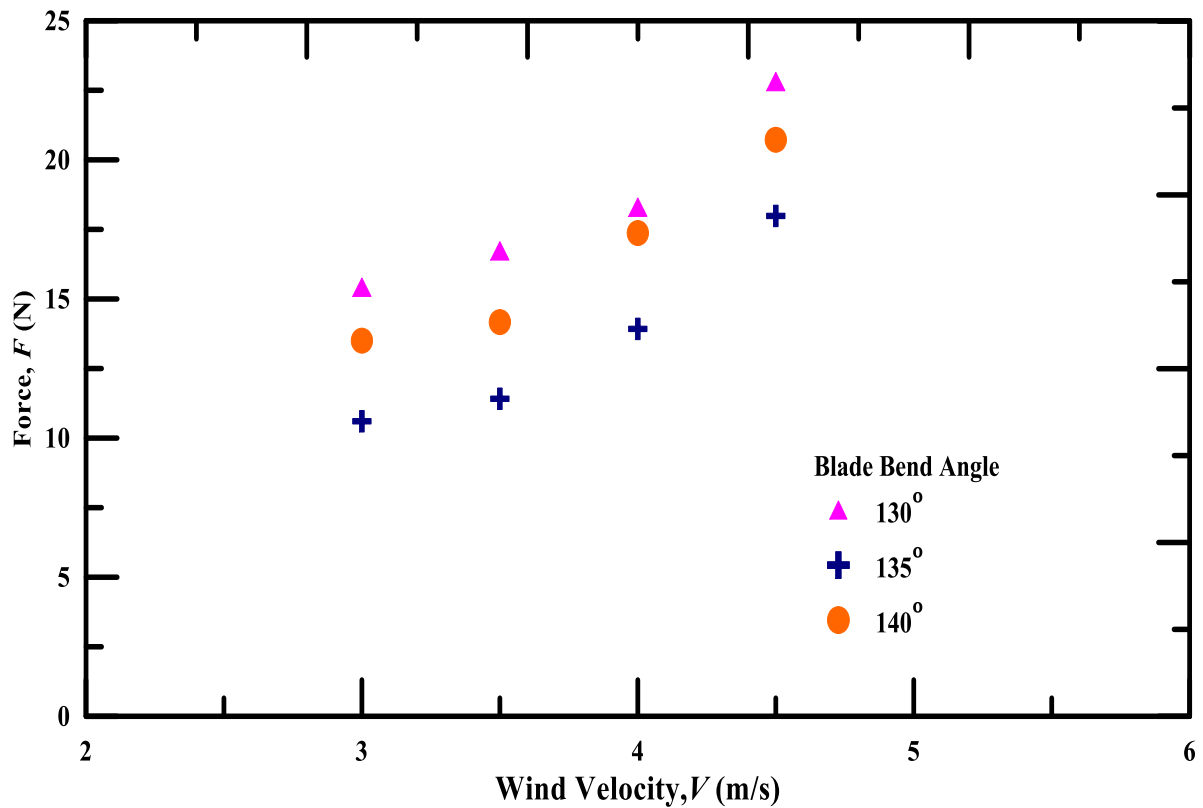


Fig. 11: Performance of rotor with different blade bend angles

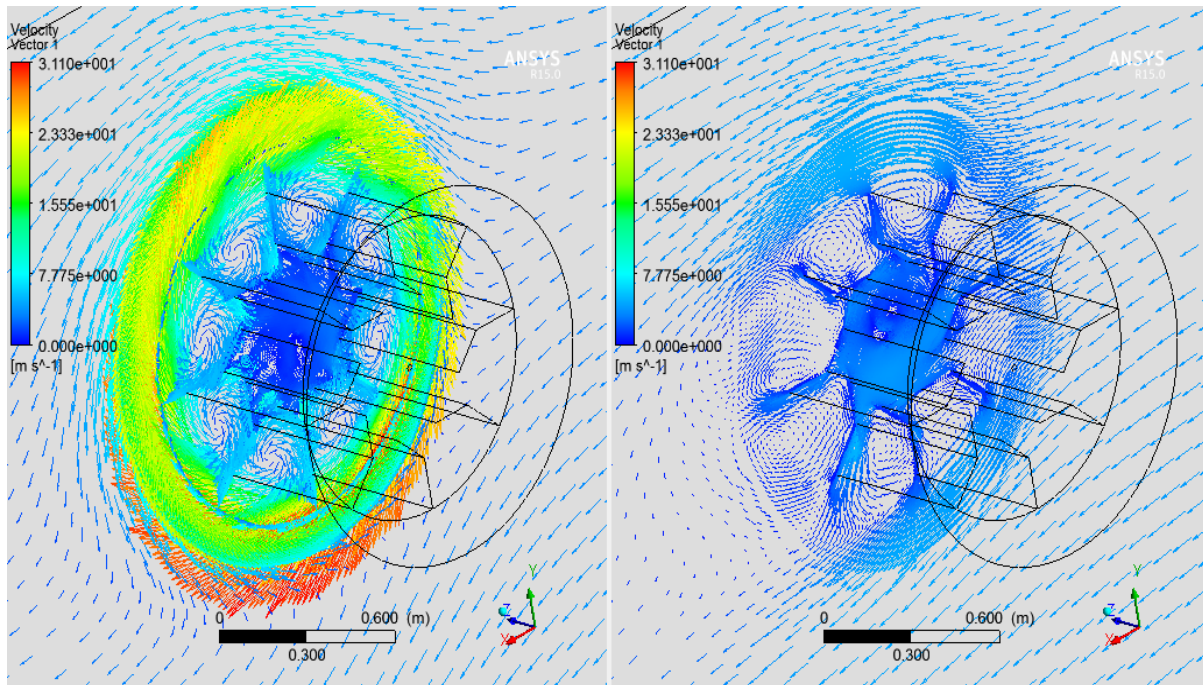


Fig. 12: Velocity vectors with MRF and without MRF

Fig. 12 shows the velocity vectors around the rotor with moving reference frame and without reference frame, this indicates the reason for using the rotating frame it can be seen from the vectors that because of the rotations of a rotating frame a swirl is created around

the blades this forces the wind to again enter the frame so that it can be utilized again. Fig. 12 also indicates that the maximum reached velocity in case of a rotating frame.

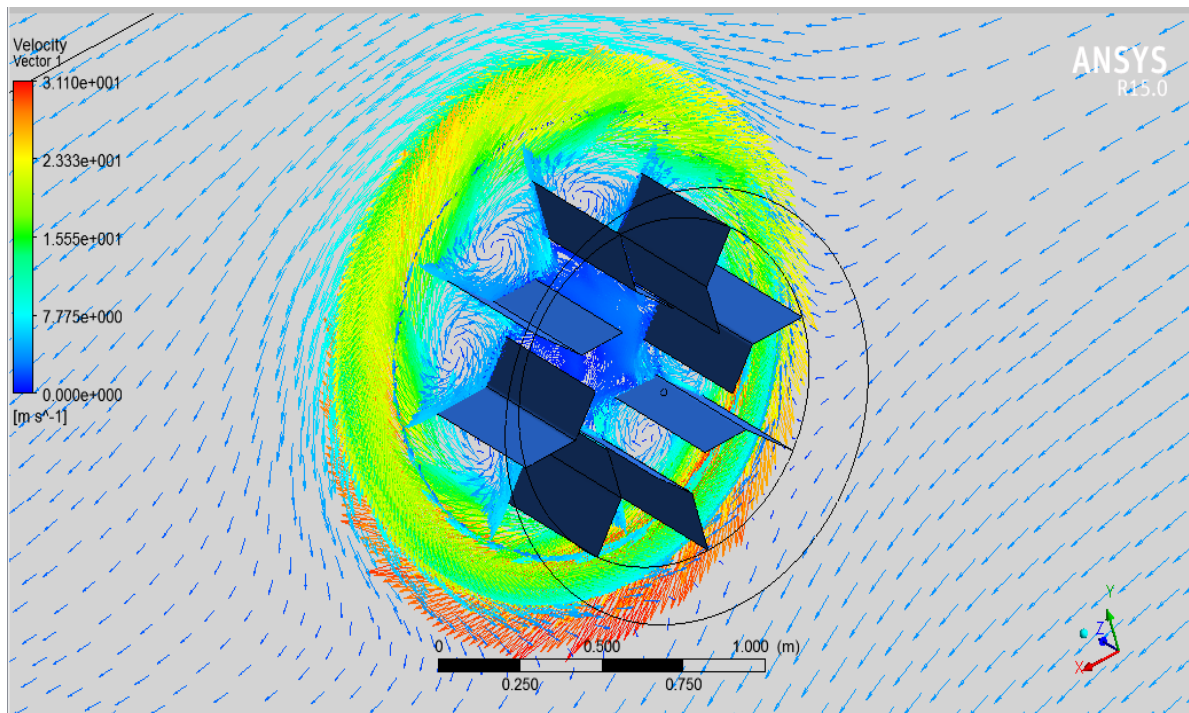


Fig. 13: Velocity vectors for a rotor with bend angle 135° wind velocity 4 m/s

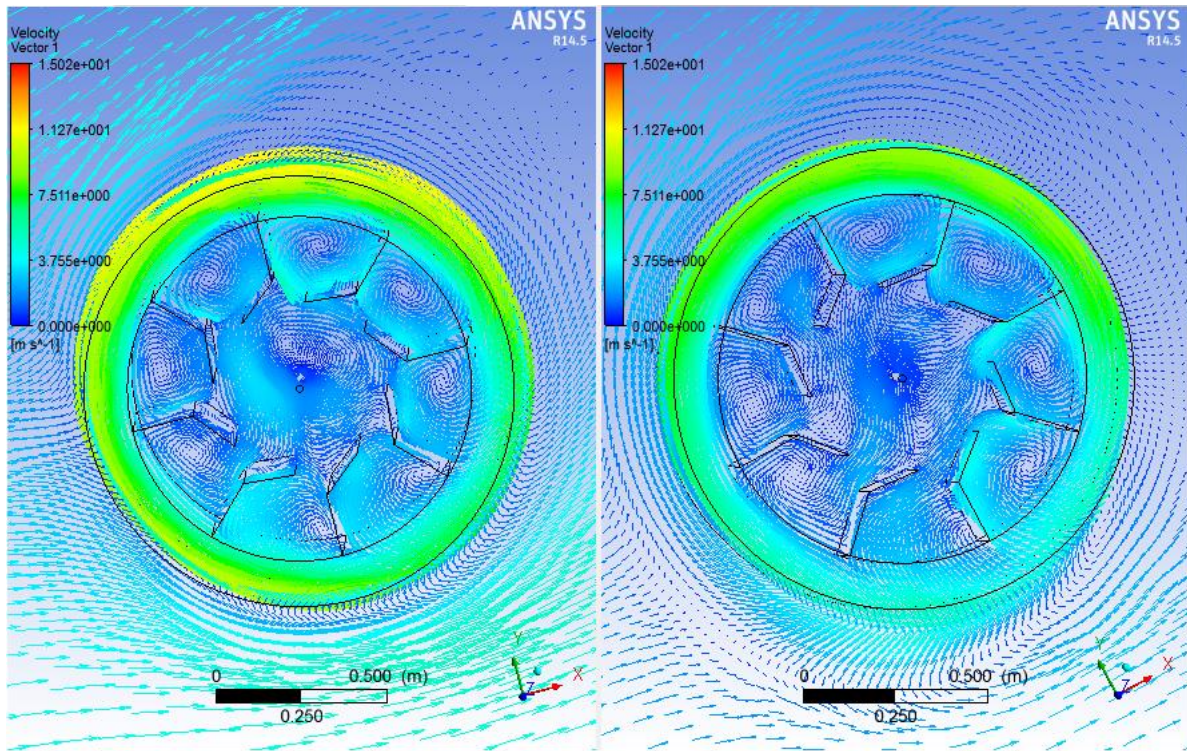


Fig. 14: Velocity vectors for a rotor with bend angle 130° wind velocity 4.5 m/s and 3 m/s

It is seen from fig. 13 that the velocity magnitude near rotor blades is small, with a no-slip boundary condition. Velocity values on the windward side of a turbine are quite high. On the rear side of the turbine, velocity is

much smaller compared to the front side. At the turbine core, the velocity distribution is not uniform. During accelerating, condition velocity magnitude is quite high compared with normal conditions.

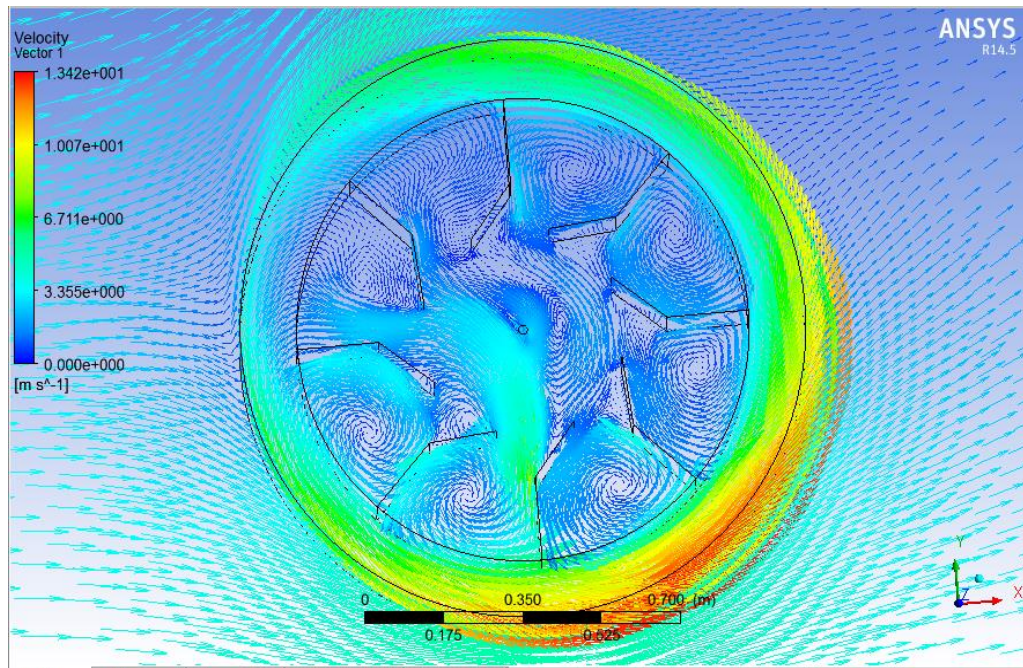


Fig. 15: Velocity vectors for a rotor with bend angle 140° wind velocity 4 m/s

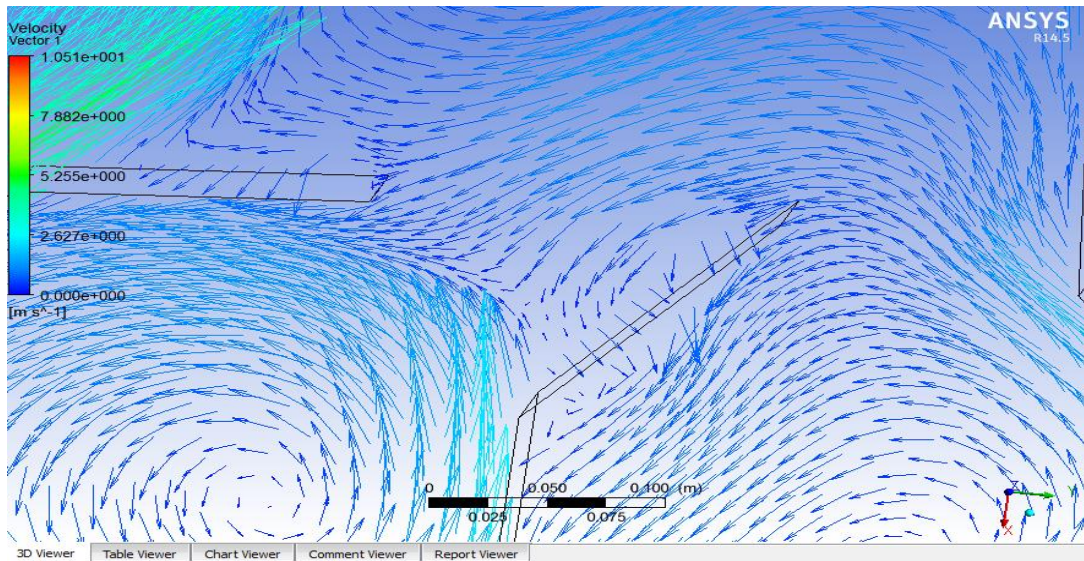


Fig. 16: Blade bend angle justification

A fan-type rotor with a certain bend angle is so selected that it creates a swirl flow in and around the blade when air strikes the rotor. It can be evident from the above fig. 16, the airflow initially strikes the first half portion of the blade where it gets deflected towards the next

half portion of the blade creating the swirl flow. Due to this swirl flow wind without leaving the moving reference zone it re-enters in the domain and gets interacted with the next adjacent blade where a similar phenomenon is created.

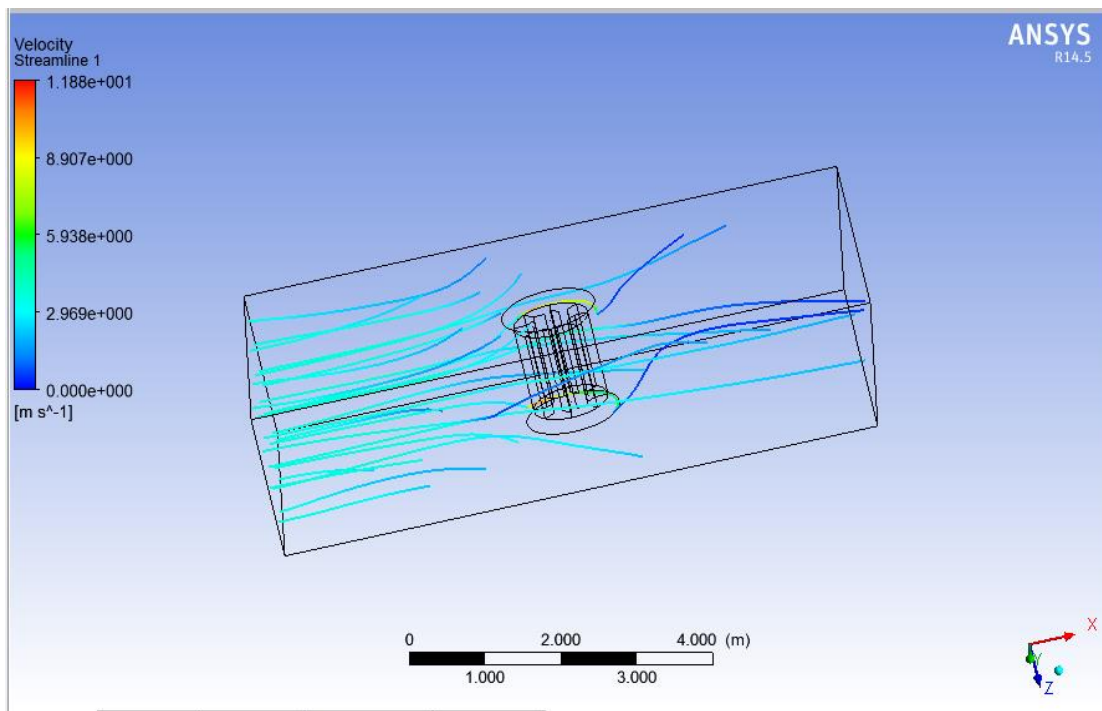


Fig. 17: Streamlines for rotor with blade bend angle 130° at 3.5 m/s

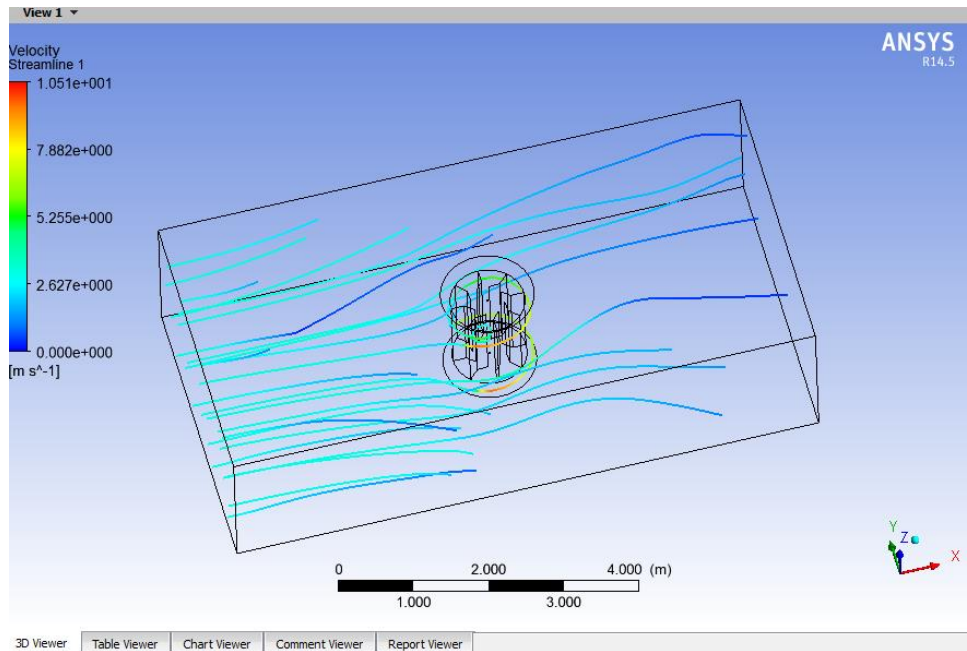


Fig. 18: Streamlines for rotor with blade bend angle 140° at 3 m/s

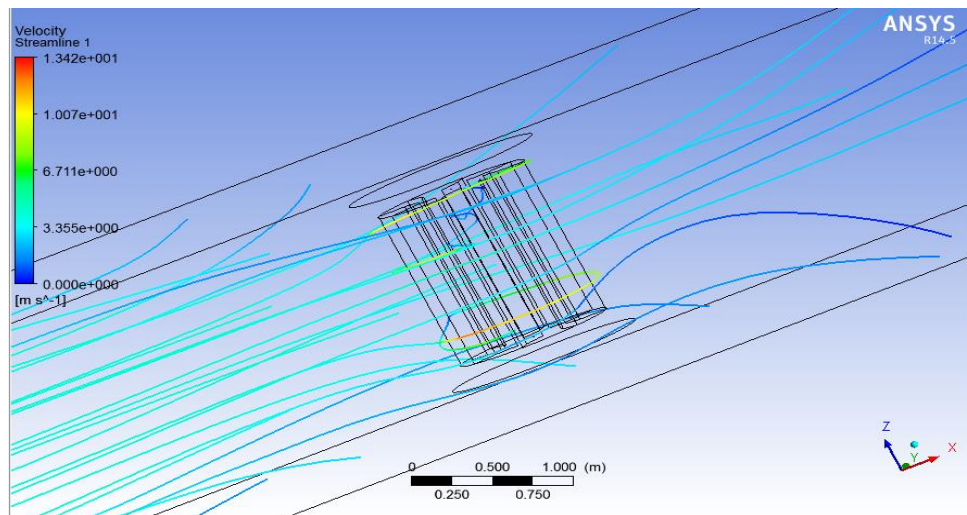


Fig. 19: Streamlines for rotor with blade bend angle 135° at 3 m/s

Fig. 17 to 19 shows the streamlines of wind flow over the turbine for the different cases. As discussed in earlier chapters that the wind turbine performance is dependent upon the physics of its ability to capture the wind from all possible directions can give better performance. As can be observed from the above figures 17, 18, 19 the rotor with blade bend angle 135° can capture the wind from all possible directions as compared to the rotor with blade bend angle 130° and 140° . This results

in the overall performance of the turbine as it can give more RPM at available wind speed.

From the streamlines of all three configurations, it can be observed that wind lines are leaving the control volume at the top, bottom, and sidewalls of control volume and finally it leaves at the outlet of control volume which indicates the fact of pressure outlet as boundary conditions at these parts of a control volume. In case, if boundary conditions at the top, bottom, and sidewalls of the rotor would have been kept as non-slip wall the wind which is leaving at these points would have again entered the control volume causing the reverse flow of the wind inside the control volume. The reverse flow in a control volume can create a negative effect on the performance of the turbine.

VI. CONCLUSION

Experimental analysis is carried out with two different blade shapes i.e. U shapes blade profile and fan type blade profile with blade bend angle 135° with a constant swept area and number of blades. The two are analyzed to find its capacity to generate more RPM at available wind speed. These configurations are tested for startup wind speed and cut-in wind speed.

During the test, it is observed that:

- The rotor with fan type blade having the bend angle started rotating at around 1.5 m/s wind speed whereas U-shaped required 2 m/s for the startup.
- Startup wind speed which is a crucial factor in the design of wind turbine is high for the U- shaped blade profile than the Fan-type blade profile.
- This indicates the effectiveness of these two over Horizontal Axis Wind Turbine (HAWT) for which the startup wind speed is above 3.5 m/s.

From the performance curves, it can be concluded that:

- It can be concluded that in both the configurations, the alternator started generating the current at around 3 m/s to 3.5 m/s which is a cut in wind speed for all HAWT.
- However, in comparison of the two tested configurations Fan type blade profile sounds effective than the U- shaped blade profile as with this blade profile it started generating the current at 3 m/s whereas for U- shaped profile it was recorded as 3.5 m/s.
- Maximum power generated by Fan type blade rotor is recorded as 203.34 Watts

CFD analysis of fan type blade profile is carried out with blade bend angle 135° and is validated with experimental values. After validation, two more Fan type blade profiles

are analyzed in CFD for their capacity to capture the wind and the force experienced by the blades.

From the CFD analysis, it can be concluded that:

- Velocity values are quite high on the windward side of the turbine. Velocity values are much smaller at the rear of the turbine compared to the front end.
- The rotor with blade bend angle 135° can capture the wind from all possible directions as compared to the rotor with blade bend angle 130° and 140° .
- Rotor with blade bend angle 135° experienced less resistance at available wind speed this indicates that it can provide more rotations than the other two.

REFERENCES

- [1] Travis J. Carrigan, Brian H. Dennis, Zhen X. Han, and Bo P. Wang, "Aerodynamic Shape Optimization of a VAWT Using Differential Evolution," ISRN Renewable Energy Volume 2012, Article ID 528418.
- [2] Abdulkadir Ali, Steve Golde, FirozAlama, and HazimMoriaa, "Experimental and Computational Study of a Micro Vertical Axis Wind Turbine," (IEF-IEC2012) Procedia Engineering 49 (2012) 254 – 262.
- [3] W.T. Chong, A. Fazlizan, S.C. Poh, K.C. Pan, W.P. Hew, F.B. Hsiao, "The design, simulation and testing of an urban vertical axis wind turbine with the omni-direction-guide-vane," Applied Energy 2013.
- [4] S. McTavish, D. Feszty, T. Sankar, "Steady and rotating computational fluid dynamics simulations of a novel vertical axis wind turbine for small-scale power generation," Renewable Energy 41 (2012) 171-179
- [5] HuiminWanga, JianliangWanga, JiYaoa, WeibinYuanb, Liang Cao, "Analysis on the aerodynamic performance of vertical axis wind turbine subjected to the change of wind velocity," Procedia Engineering 31 (2012) 213 – 219
- [6] MdNahid Pervez and WaelMokhtar "CFD Study of a Darreous Vertical Axis Wind Turbine" Grand Valley State University, Grand Rapids, MI 49504
- [7] Sukanta Roy, Ujjwal K. Saha, "Computational study to assess the influence of overlap ratio on static torque characteristics of a vertical axis wind turbine," Procedia Engineering 51 (2013) 694 – 702.
- [8] Habtamu Beri, Yingxue Yao, "Double Multiple Stream Tube Model and Numerical Analysis of

- Vertical Axis Wind Turbine,” Energy and Power Engineering, 2011, 3, 262-270
- [9] Joachim Toftegaard Hansen, Mahak Mahak, Iakovos Tzanakis, “Numerical modelling and optimization of vertical axis wind turbine pairs: A scale up approach,” Renewable Energy 171 (2021) 1371-1381
- [10] Sayyad Basim Qamar and Isam Janajreh, “Investigation of Effect of Cambered Blades on Darrieus VAWTs,” Energy Procedia 105 (2017) 537 – 543
- [11] David Wafula Wekesa, Churchill Otieno Saoko, Joseph Ngugi Kamau, “An experimental investigation into performance characteristics of H-shaped and Savonius-type VAWT rotors,” Scientific African 10 (2020) e00603
- [12] M. Salman Siddiqui, Muhammad Hamza Khalid, Rizwan Zahoor, Fahad Sarfraz Butt, Muhammed Saeed, Abdul Waheed Badar, “A numerical investigation to analyze effect of turbulence and ground clearance on the performance of rooftop vertical axis wind turbine,” Renewable Energy 164 (2021) 978-989.
- [13] Jabir Ubaid Parakkal, Khadije El Kadi, Ameen El-Sinawi, Sherine Elagroudy, Isam Janajreh, “Numerical Analysis of VAWT wind turbines: Joukowski vs classical NACA rotor’s blades,” Energy Procedia 158 (2019) 1194-1201.
- [14] Mukesh Kumar Rathore, Meena Agrawal, Prashant Baredar, “Energy production potential from the wake of moving traffic vehicles on a highway by the array of low economic VAWT,” Materials Today: Proceedings in Press
- [15] T. Micha Premkumar, Seralathan Sivamani, E. Kirthees, V. Hariram, T. Mohan, “Data set on the experimental investigations of a helical Savonius style VAWT with and without end plates,” Data in Brief 19 (2018) 1925–1932



Dr. Prashant W. Deshmukh is currently associated with the College of Engineering, Pune, India as a faculty in the Mechanical Engineering Department. He acquired his Ph.D. from IIT Bombay, India. He has been involved in academics for the past 16 years and involved in several projects for passive heat transfer augmentation techniques. He has published 6 journal articles in Scopus indexed journals.



Mr. Shrikant D. Hade is currently associated with Pune Institute of Computer Technology, Pune-43, India as a faculty of Mechanical Engineering in the First Year Engineering Department. He has completed his M.E, from MIT-COE, Pune. He has been involved in academics for the last 9 years.



Mr. Hrushikesh M. Hiwase is currently associated with Pune Institute of Computer Technology, Pune-43, India as a Workshop Superintendent. He has completed his M.E, from Government College of Engineering, Karad. He has been involved in academics for the last 17 years.